Biomimetic Mineralization in and on Polymers

Paul Calvert*

Arizona Materials Laboratories, University of Arizona, Tucson, Arizona 85712

Peter Rieke

Battelle Pacific Northwest Laboratories, Richland, Washington 99352

Received February 14, 1996. Revised Manuscript Received May 3, 1996[⊗]

Biological mineralization leads to the development of finely scaled, highly controlled inorganic precipitates in organic matrixes. It was initially thought that this control was mainly exercised through lattice-matching epitaxy between the protein or polysaccharide matrix and the mineral. We discuss the importance of such heterogeneous nucleation versus other forms of kinetic control of mineralization. We review progress in synthetic systems for mineralization from solution at Langmuir monolayers and Langmuir−Blodgett films, at surface-adsorbed monolayers and in polymer films.

Introduction

In biomineralization, inorganic precipitates form under the full control of an organic tissue matrix. This control includes manipulation of local concentrations of the precipitants, the presence of nucleating surfaces and the presence of inhibitors in solution which can bind to specific faces on the growing mineral. Particle size, shape and orientation are regulated by the matrix. Such in situ deposition processes also avoid the difficulties of handling nanosized particles while avoiding aggregation and without the need for large amounts of surfactant to keep them in suspension.

This review discusses biomimetic routes to the formation of composites containing nanometer particles and of device structures based on patterns of nanosized particles on surfaces. This approach can be compared with biomineralization processes and has the potential for providing much greater control of particle morphology and distribution than would conventional blending or deposition methods.

Prospects for Composites with Nanoparticle Reinforcement

One goal of in situ mineralization is the formation of composite materials with properties comparable to those of bone and similar hard tissues.[1] These materials comprise a tough collagen matrix, reinforced with up to 50 vol % of ribbonlike hydroxyapatite crystals. These ribbons are a few nanometers thick and up to a micron long. The modulus of bone is up to 30 GPa, about 10 times that of a hard polymer, while the strength is up to 200 MPa and the material is tough.[2] Reinforced polymers, with increasing volume fractions of particles, do not usually reach moduli above 10 GPa before the material becomes brittle and weak. Such composites contain reinforcing particles on the scale of several microns rather than nanometers.

In theories of composite materials there is no primary link between the size of the reinforcing particles and mechanical properties. Hence nanocomposites should not be superior to conventional composites with micron-sized particles. However, molding and extrusion may be viable with finer reinforcing particles.

Synthetic composite materials are produced by the blending of reinforcing fibers or particles with resins. For improved strength and greatest stiffness, particles should have an aspect ratio of 100−1000. Synthetic fibers have diameters of 8−10 μm, thus requiring fibers to be 1−10 mm long. This requirement is met in continuous fiber composites, but the high cost of processing these materials has put emphasis on cheaper processing methods such as extrusion and molding of short-fiber composites. Normal extruders break down long particles so that it is hard to get good reinforcement. Fibers with diameters in the nanometer range could have a high axial ratio without being vulnerable to fracture during processing.

Nanoparticles may also affect composite properties by modifying directly the properties of the matrix material. Existing rubber formulations use carbon black and fumed silica nanoparticles. There is evidence that the effective volume fraction of these fillers is higher than the actual volume fraction, because a significant proportion of the polymer is immobilized by being attached to the particle surfaces. This may also be the source of the high elastic moduli of hybrid organic−inorganic nanocomposites above their glass transition temperature.[3]

Nanoparticle composites cannot be processed by conventional methods involving suspensions of particles in liquids or low-viscosity resins. As particles become finer, colloidal forces become relatively more important and it becomes more difficult to achieve unagglomerated dispersions at high volume fractions. One solution to this difficulty is to use very high shear forces, as in milled rubber. A second approach, where possible, is to use large amounts of dispersant and restrict the system to low volume fractions, at least while it is fluid. A third approach, underlying this review, is to avoid dispersing a preformed reinforcing phase and instead to grow the particle phase in the matrix or on the surface where it is needed. This is a biomimetic

[⊗] Abstract published in *Advance ACS Abstracts,* July 15, 1996.

S0897-4756(96)00126-3 CCC: $12.00

approach in that mineralized biological structures generally form by growth in situ rather than by transport of preformed particles. In this approach there is the possibility of close control of particle size, shape, orientation, and locality. A brief look through any survey of biomineralization will suggest many complex multifunctional structures that should be formable.[4]

Optical properties is one area where nanoparticle composites will have markedly different properties from conventional composites.[5] Scattering decreases with particle size such that it should be possible to make materials combining the toughness and transparency of glassy polymers with the nonlinear optical properties of embedded particles. For transparency, not only must the particles be nanometers in size, they must also be distributed uniformly on the scale of a micron and higher. In addition to these effects, nanoparticle-reinforced composites may be desirable, when compared to conventional composites, for the special properties of the fine particles themselves.

Prospects for Nanoparticle Films. There are a number of reasons for forming films of inorganic particles attached to a polymer surface or embedded just under the surface. Greatly reduced permeability should be achievable with dense, thin inorganic films. Surface hardening and scratch resistance have been demonstrated with attached layers of inorganic−organic hybrid, and sol−gel oxides.[6−8] Biocompatibility may be induced by titania or apatite coatings.

Inorganic films can be deposited on a polymer surface by many vapor-phase techniques. Solution methods offer the potential advantages of much cheaper equipment since vacuum apparatus is not needed. Deposition rates may be higher and environmental concerns may be milder. Possibly more important is that materials can be deposited which would not withstand high-temperature or high-vacuum processing. This may particularly apply to protein-based sensors and other compounds designed to sense mild chemical agents under ambient conditions.

In silicon technology, patterns are formed using photoresists exposed through masks. At lower resolution, patterns can be silk screened onto printed circuit boards. Mineral patterns in biology often form by selective growth on particular organic substrates. There are examples of similar selectivity in CVD[9] and in electroless plating. In addition, it should be possible to form device structures on surfaces if patterned films of different materials can be formed.

Biomineralization

Biomineralization occurs in many forms with different degrees of structural control. Given a supersaturated medium, mineral may form externally to the organism, as for coral[10] and many examples of bacterial mineralization. Dental plaque arises from the mineralization, by hydroxyapatite from the saliva, of a layer of adhesive polysaccharide deposited on the tooth surface by *Streptococcus mutans*.[11,12] A similar mechanism allows blue-green algae to form stromatolites by trapping of sand in a layer of mucus and then cementing this with calcium carbonate by locally raising the carbonate concentration.[13]

Coral depends on the supersaturation of seawater for calcite and aragonite into the concentration regime where the solution is metastable and does not precipitate spontaneously. This in turn depends on the carbon dioxide equilibrium between the sea surface and the atmosphere. Nucleation and growth of carbonate at the surface of the individual animals is then manipulated by provision of nucleating sites or local changes in pH or carbonate levels. The nucleating site appears to be microscopic calcite crystals which subsequently give rise to aragonite overgrowth.[10] The calcite may form intracellularly or extracellularly.

A recent paper by Keller et al.[14] discusses how, given some combinations of surface energy and volume free energy, a crystal form which is normally metastable may be the most stable for a small crystal. While this was discussed for polyethylene crystallization, similar situations may occur in many minerals, especially in the presence of surface-binding macromolecules.

Beyond these simple systems, there are many examples of mineralization which occurs within the organism but is still extracellular. These include bone, tooth enamel and dentine, mollusc, and crustacean shell.[15] Bone mineralization may involve control of phosphate levels through matrix vesicles at the mineralizing surface. These cell satellites contain high levels of phosphatases and may increase local phosphate levels by cleavage of triphosphates, such as ATP or GTP. They may also locally remove pyrophosphate ($P_2O_7^{4-}$), an inhibitor of apatite crystal growth. In addition to local control of levels of precipitating species and inhibitor, matrix proteins are thought to act as nucleating sites. Thus bone mineral forms within the collagen fibrils,[16] and this has been attributed to acid sites at the ends of the triple helixes of collagen. Certainly mineralization does accentuate the electron contrast of the $^1/_4$ stagger pattern of collagen fibrils, reflecting the regular positioning of helix end sections.

While we know a great deal about bone mineralization, we do not really understand how it is controlled. Many of the clearest studies have been on mineralizing turkey tendon, which is not really bone.[15] Unlike bone, dentine has no matrix vesicles. True bone shows distributions of mineral which change as the process proceeds. Early stages involve unoriented precipitation around the matrix vesicles and there may be a first precipitation of amorphous calcium phosphate.[17,18] Observations such as these are also often in doubt as there may be artifacts of the preparation for microscopy.

Until recently we knew little about the sequence of events in shell mineralization. Recent studies on "flat pearls" have provided a much clearer picture of the sequence of events, but not yet of the underlying mechanisms.[19] The model of nacreous shell formation is particularly interesting, both because it results in a strong laminated ceramic structure[20] and because such a layered deposition of organic and inorganic phases could be applicable to many synthetic functions as mentioned above.

The most controlled mineral structures are obtained by mineralization inside cellular vesicles. Examples are the magnetic bodies of magnetotactic bacteria and the silica or calcite enclosures of diatoms and foraminifera.[15] As nanostructures, these minerals are interesting in that they show a very high degree of shape control and very high resolution. However, even though these structures can be exported into the extracellular envi-

ronment, they are isolated particles and so do not inform us about the formation of large structures. Many sponges do form elaborately shaped spicules and then export them from the cell and fuse them to make skeletons.[21] From these structures it does seem that both crystalline (calcite) and amorphous (silica) materials can be shaped by growth in contact with a lipid membrane which presumably controls the position of deposition at any time.

Other Natural Mineralization

Natural but abiological mineralization occurs widely. Boiler scale is an important engineering problem. Loss of carbon dioxide from bicarbonate solutions (HCO_3^-) leads to increasing levels of carbonate (CO_3^{2-}) and precipitation, which is tackled by the addition of inhibiting polymers. Different materials show different tendencies to form scale. There are similar problems with the precipitation of barium sulfate during oil extraction.[22]

Petrification of plants is a well-known phenomenon. Petrified wood forms by the deposition of silica, apparently within the cellulose cell walls.

There are a number of mineralization diseases including stone formation in kidneys, bladder, gall bladder, and salivary ducts. Gout is due to the deposition of needle-shaped monosodium urate into the articular cartilage and their subsequent release into the joint space, which causes an inflammatory response.[23] In gout patients, the body is essentially uniformly supersaturated with respect to urate. However, precipitation is selective for the articular cartilage, suggesting a strong matrix effect. Since sodium urate has a very polar surface and cartilage has a high concentration of anionic polysaccharides, this association seems rational.

Control of Crystallization

Crystal growth is conventionally divided into nucleation and growth stages. The growth mechanism is the same in both stages in that individual molecules or ions add to sites at an existing surface or cluster. However, during nucleation the high surface-to-volume ratio means that the cluster is increasingly more stable than the surrounding solution (Figure 1a). During growth, the energy of the crystal or cluster decreases continuously. Observations of nucleation kinetics seem to correspond well to simple Monte Carlo computer models of cluster formation by stochastic addition and loss of atoms.

Homogeneous and Heterogeneous Nucleation. An organic surface may play many roles in promoting mineral deposition. These include physisorption of ions and colloidal precipitates, orientation of crystal lattices, preferential deposition of particular crystal phases and, last but not least, heterogeneous nucleation. Of these, how the surface influences nucleation is the least studied and the most misinterpreted. The preferential or oriented deposition of a mineral phase on a surface is often interpreted to imply heterogeneous nucleation. This may not be so. In, for example, the case of $CaCO_3$ nucleation under L−B films, highly oriented crystals can be obtained.[24] But nucleation is driven by the evolution of CO_2 at the air−water interface and occurs even in the absence of a L−B film. The L−B film

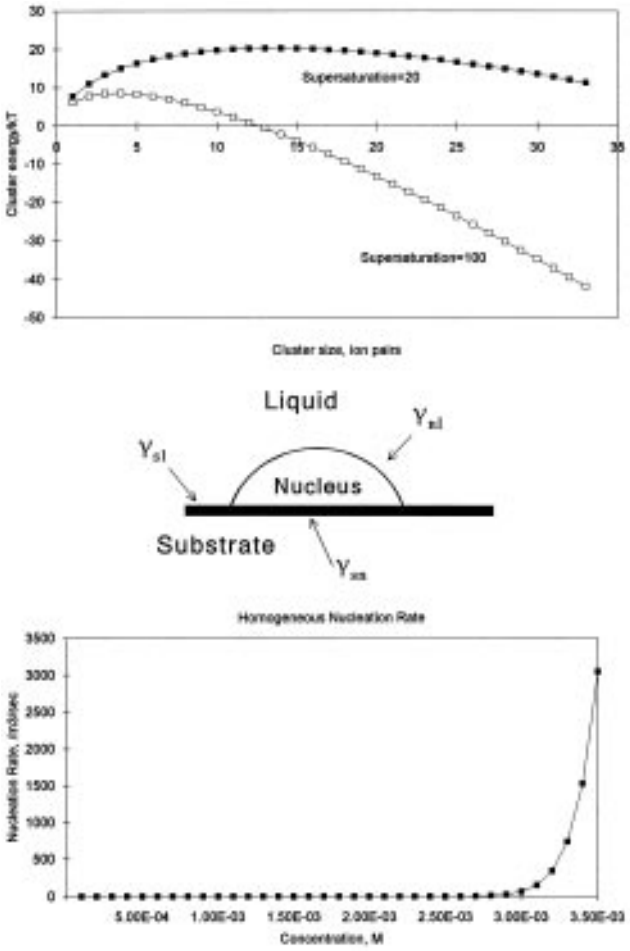

Figure 1. (a, top) Plot of nucleus energy versus cluster size for calcium oxalate in aqueous solution at two supersaturations; (b, middle) schematic heterogeneous nucleus; (c, bottom) plot of homogeneous nucleation rate versus supersaturation for calcium oxalate.

modifies nucleation and growth but does not induce nucleation. For submerged solid substrates, homogeneous nucleation can result in formation of colloidal particles. The forces involved in physisorption of colloidal particles are sufficient to cause orientation of the crystal lattice and preferential stabilization of mineral phases.[25]

Nucleation theory has been reviewed elsewhere numerous times.[26−29] The starting point for both heterogeneous and homogeneous nucleation is that the free energy for formation of a cluster of size n, in a solution of supersaturation S, is given by the balance between the energy gained by formation of bulk phase, (kT ln(S) per molecule) and the energy required to form new surface area. The former scales as the embryo radius cubed and the latter as the radius squared. The equation is

$$\Delta G = -nkT \ln(S) + \sigma A \qquad (1)$$

where σ is the interfacial free energy for nucleation (IFEN), and A is the surface area of the nucleus. For homogeneous nucleation, the IFEN is equivalent to the interfacial free energy of the nucleus/liquid interface, γ_{ln}. This parameter is sometimes referred to as the surface tension—a terminology which is misleading when referring to a solid and especially so when the nucleus is very small. For heterogeneous nucleation the

IFEN is given by the sum of the nucleus/liquid and nucleus/substrate interfaces formed and the liquid/substrate displaced by the nucleus Figure 1b:

$$\sigma = \gamma_{nl}\xi + (\gamma_{ns} - \gamma_{ls})(1 - \xi) \quad (2)$$

ξ is the ratio of the nucleus/liquid area to the whole area, A_{nl}/A.

In this form eq 1 can be manipulated to give the free energy of formation of the critical nucleus:

$$\Delta G^* = \beta\nu^2\sigma^3/(kT\ln(S))^2 \quad (3)$$

using geometric arguments relating volume to surface area, assuming a constant shape, and, very importantly, assuming that the IFEN is independent of particle size. β is a shape factor and ν is the molecular volume. Equation 3 is applicable to either homogeneous or heterogeneous nucleation, provided the difference in the definition of the IFEN is recognized.

The normal approach for heterogeneous nucleation is to assume a spherical cap nucleus.[26,27] Young's equation

$$\gamma_{ls} - \gamma_{ns} = \gamma_{nl}\cos\theta \quad (4)$$

is substituted into eq 2 to eliminate γ_{ns} and γ_{ls} and, after some manipulation, the free energy for formation of the critical nucleus is given by

$$\Delta G^*_{het} = \Delta G^*_{hom}(1 - \cos\theta)^2(2 + \cos\theta)/4 = \Delta G^*_{hom}\Gamma(\theta) \quad (5)$$

where the latter term, $\Gamma(\theta)$, is only a function of the contact angle of the spherical cap nucleus with the substrate. Nyvlt et al.[27] refer to $\Gamma(\theta)$ as an adjustable parameter. There are objections to the use of eq 5 as it masks the contribution of the substrate in inducing nucleation. Our objective is to understand the contribution of the substrate in promoting mineral deposition.

As shown in Figure 1a for calcium oxalate solution, a plot of eq 1 versus n is reminiscent of an activation energy barrier—although we have adapted a thermodynamic rather than a kinetic discussion. The transition state is the critical nucleus size. Particles larger than this tend to grow into crystals and particles smaller than this tend to dissolve. Consequently, eq 3 (or with minor differences, eq 5) is substituted into the Arrhenius equation to get an expression for the rate of nucleus formation, Figure 1c. The preexponential factor was taken as 10^{24} m^{-3} in Figure 1c. This factor is notorious for showing very large discrepancies between theory and experiment but makes little difference to the supersaturation at which nucleation is observed. Nucleus formation requires higher supersaturations than crystal growth. Once a certain density of nuclei are formed the supersaturation drops and crystal growth dominates.

Given this S-shaped curve for extent of crystallization versus time, the induction time for crystallization, t_{ind}, is a very convenient measure of nucleation rates. This is the time required for clear evidence of the onset of crystal growth and can be given by

$$\tau_{ind} = N^*/J \quad (6)$$

where N^* is the nucleation density, at the onset of obvious crystallization, and J is the nucleation rate.[27] To relate the induction time to nucleation rate, it is also necessary to know the number density of crystals, N. Alternatively the induction time can be taken as the time for a certain fraction of crystallization to occur, for instance, 10% or 50%. In this case the induction time is dependent on both the nucleation and growth rates. For interface-controlled growth on a surface, the induction time would depend on $1/J^{1/3}$, whereas for diffusion-controlled growth on a surface, the induction time would depend on $1/J^{3/5}$.[26,27] The well-known Avrami analysis treats the same problem for melt growth.

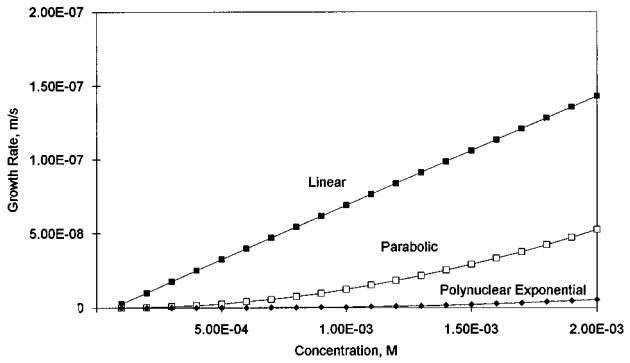

Figure 2. Schematic plot of growth rate vs supersaturation for linear crystal growth kinetics, parabolic (dislocation controlled) kinetics, and polynuclear surface nucleation kinetics. Parameters for calcium oxalate monohydrate.[38]

Another induction time is defined in the nucleation literature, which is the time lag for an embryo to first grow to the critical size, microseconds in normal liquids.[28]

While the IFEN allows comparison of the efficacy of different surfaces to induce nucleation, it does not provide much insight to the particular surface physical and chemical characteristics that control the IFEN. It is necessary to compare the IFEN to other measures of surface properties such as chemical composition, adsorption isotherms, and wettability by various solvents. A major problem is that theoretical connection between the interfacial free energies and the above surface properties is lacking. One approach is to use the wettability theory of Van Oss and Good to obtain independent measurement of the surface free energies contributing to the interfacial free energies of eq 3.[30,31]

Crystal Growth: Interfacial Kinetics. The fundamental process of crystal growth is the addition of molecules to a surface. In the relatively simple case of growth from a pure melt, such as ice formation from water, the thermodynamic driving force is simply related to the supercooling, $\Delta T = T_m - T$. In simple symmetrical materials, such as many metals or camphor, the rate of growth (in mm/s) is proportional to the undercooling (Figure 2)[32] and the growing crystal shows no facets.

In less symmetric systems, such as silicon, surface energy is more important and the growing crystal shows facets. On these flat surfaces the growth rate is proportional to the square of the supercooling and most addition of new atoms occurs at steps associated with the emergence of screw dislocations at the surface, according to the BCF (Burton—Cabrera—Frank) model.[33] Still less symmetrical molecules, such as orthoterphenyl, show facetted growth faces where each new layer of crystal is nucleated by the formation of a disk-shaped cluster on the previous flat surface. The resulting growth rate is exponentially dependent on super-

saturation (Figure 2). These three mechanisms of crystal growth have been supported by computer modeling and observations by optical and electron microscopy and by atomic force microscopy.[34−37]

Crystal growth kinetics of salts from solution have been reviewed by Nielsen,[38] who gives rules that can be used to estimate rates in many systems. In comparing growth rates for salts of different cations, the loss of water of hydration from cations is believed to be a major barrier limiting growth rates. Most salts follow a square-law dependence of growth rate on supersaturation.[38] For this square-law model, supersaturation is expressed as $(c/s - 1)$, where c is the salt concentration and s is the saturation concentration. In other models, supersaturation is expressed as $\ln(c/s)$.

If growth is controlled by simple interface kinetics, the rate is dependent on supersaturation but not on the ratio of the two ions.[39] If diffusion is controlling (see below), the rate is dependent on the concentration of the most dilute ion. A simple chemical kinetics treatment of crystal growth would give a rate dependent on $(c/s)^2$ for a binary salt, which has led to many treatments being cast in terms of addition of ion pairs or other clusters coupled with a conventional kinetic constant. In most cases ion pairing is not important, but this does affect the growth rate of calcium carbonate.[39] Also many growth rates are measured by weight increase of a collection of seed crystals with known surface area. Results in terms of mol m^{-2} s^{-1} must be converted into mm s^{-1} for comparison with microscopic measurements.

Even with the above uncertainties, we can make reasonable predictions of growth rates for many salts from aqueous solution as a function of supersaturation.

Crystal Growth: Diffusion Effects. The discussion of interface kinetics above assumes that the concentration of ions in solution near the growing crystal is the same as in the bulk solution. This is normally untrue in dilute solutions and diffusion of ions becomes a limiting factor on crystal growth. In growth rate measurements, diffusion gradients may be suppressed by rapid stirring or attachment of the crystal to a spinning plate.[27,40] If we can estimate the thickness of the unstirred diffusional boundary layer adjacent to the crystal surface, we can calculate the extent of depletion corresponding to any given crystal growth rate.

For small crystals in liquid, the boundary layer thickness is often taken as being equal to the crystal radius. It is often then useful simply to compare the actual interfacial growth kinetics with the maximum mass diffusion rate, for the case where the concentration of ions at the interface is reduced to saturation by rapid incorporation into the crystal. Either interfacial kinetics or diffusion can then be defined as limiting.

In other cases we do not know the thickness of the diffusive boundary layer, since this depends on the extent of stirring and convection. In a gel medium, convection can be ignored and the linked diffusion and growth problem solved directly.

It should be noted that only the crystallizing species are depleted. In the case of calcite growth, for instance, the bicarbonate/carbonate equilibrium results in excess bicarbonate at a pH below 10. If the species equilibrate rapidly, the limiting diffusion is that of bicarbonate. If not, it is that of carbonate.

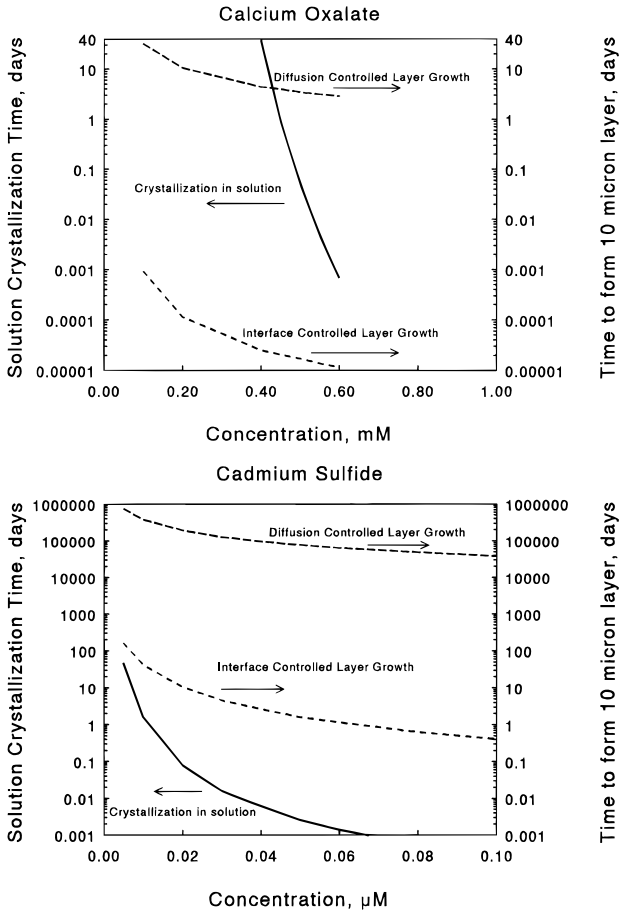

Figure 3. (a) Concentration window for controlled growth of calcium oxalate on a nucleating substrate. (b) Concentration window for controlled growth of cadmium sulfide on a nucleating substrate.

If we take the example of calcium oxalate, for which we have studied mineralization processes,[41,42] the growth rate, following Nielsen,[38] is given by

$$\nu = k_2(s-1)^2 \qquad k_2 = \frac{0.1\alpha\nu_i K_{ad} V_m c_s}{\gamma/kT \exp(\gamma/kT)}$$

$$k_2 = 5.57 \times 10^{-11} \text{ m s}^{-1}$$

where s is the saturation (c/c_s).

Control of Crystal Growth. Consider a surface, which is to be coated with a layer of mineral, immersed in a salt solution. Given expressions for nucleation rate and crystal growth rate as a function of supersaturation, it is possible to define a region where controlled mineralization is possible (Figure 3a). This region will be defined by the saturation concentration, as a minimum, and the concentration at which spontaneous nucleation and growth occurs before any substantial addition to a surface has occurred, as a maximum. In Figure 3a, this is limited to the area at the top left of the plot, above the diffusion-controlled growth line and below the crystallization-in-solution line. Films 10 μm thick would take at least several days to grow.

Assume also that we coat the surface with a perfect heterogeneous nucleator, so that crystal growth commences immediately. The maximum growth rate of the surface layer is then the maximum growth rate achievable in a solution at the upper boundary of supersaturation. For systems of low solubility, diffusion limita-

tions cause this rate to be very slow. For device structures 1 nm/min could be useful, while for barrier films 1 μm/min would be more reasonable, and mechanical composite structures should be grown 10−100 times faster than this.

As shown in figure 3a, to grow crystals on an already nucleated surface, without spontaneous nucleation of new crystals in solution, requires a concentration of below 5×10^{-4} M. For a 1 μm or 1 mm crystal growing in this solution the interfacial growth rate is 2.7×10^{-9} m s^{-1} but the diffusion-limited growth rates would be 3.2×10^{-8} and 3.2×10^{-11} m s^{-1} assuming a high pH where all the oxalate exists as $(COO)_2^{2-}$. Hence small crystals will grow at a rate limited by interface kinetics, but larger crystals and surface films will grow at a rate limited by diffusion. This "either interface or diffusion" analysis is clearly a simplification of compound control of the growth rate but will be accurate at the extremes.[26]

Cadmium sulfide (Figure 3b) is much less soluble than calcium oxalate and the conditions for deposition of a surface film require impracticably slow growth, taking above 10^6 days to form a 10 μm layer.

There are a number of approaches to moving this window to a more tractable region. Diffusional effects can be reduced by increasing the available solute concentration without changing the supersaturation. Thus, reducing the pH will increase the total oxalate concentration, while keeping the same concentration of the precipitating species $(COO)_2^{2-}$. As long as oxalic acid and $(COOH)-(COO)^-$ quickly equilibrate with the dianion, the effective surface concentration will be increased. The same reasoning applies to sulfides and carbonates. Similarly the effective Ca^{2+} concentration can be increased by complexation with EDTA or other ligands.

Since mineralization can be regarded as a competition between surface precipitation and precipitation in solution, the process can be favored by limiting the supersaturated zone to a thin layer adjacent to the surface. This also increases the chance that growing clusters collide with the surface and become incorporated.

The ratio of diffusion coefficient to growth rate defines a characteristic distance for a crystallization process. With aqueous ion diffusion coefficients of about 10^{-5} cm^2 s^{-1}, a growth rate of 1 μm s^{-1} would give a distance of 1 mm. Thus the local generation of precipitants can restrict mineralization to the vicinity of a surface.

This localization can be achieved by diffusion of one reactant through the interface,[43] by the attachment of catalytic species to the interface (Bond, G. M., *Mater. Sci. Eng. C*, in press) or by photogeneration of precipitants or acidity. It may be that some oxide or semiconducting precipitates are intrinsically catalytic for the dehydration or oxidation of aqueous ions.

Precipitation can be suppressed by addition of small concentrations of inhibitors to the solution. The design of inhibitors has been discussed, one successful approach is to form a bidentate ligand with two groups similar to the precipitating anion or molecule and coupled by a flexible linkage.[44,45]

Polymeric inhibitors can be excluded from surface regions which carry an attached polymer layer. As a result, precipitation at a polymer surface can be favored over precipitation in solution.[42,46−48] Bone mineralization may be controlled, in part, by pyrophosphate acting as an inhibitor. This compound is continuously produced and destroyed in normal tissue. Mineralization is then induced by locally enhanced enzymatic hydrolysis of pyrophosphate.[23]

Mineralization under L−B Films and at Interfaces

Mineral growth at organic surfaces differs substantially from that at inorganic surfaces. Extensive work in the latter case has shown that epitaxial lattice matching is the most important criterion determining whether an overgrowth will deposit in registry with a particular substrate.[49] Simple calculation of the lattice mismatch is a very good predictor of success in epitaxial growth. Organic surfaces, on the other hand, have a much higher degree of structural flexibility and may have strong surface-specific binding forces, such as the ability of the functional groups to chelate metal ions. Further structural or epitaxial relationships can involve simple geometric matching of lattices as well as stereochemical matching of bonds between substrate and overgrowth. It is not yet clear what relative contribution each has in promotion of nucleation and oriented growth of the mineral phase. In the following review of the literature, we try to emphasize how a particular study addresses this issue.

Studies of nucleation and growth of minerals on organic substrates fall into two categories based upon the type of information sought. Many if not most studies attempt to show some epitaxial relationship between the substrate and the mineral overgrowth. Various ways of changing the structure of the organic substrate are induced and correlated with the orientation of the overgrowth. Such studies are very amenable to mineralization under Langmuir−Blodgett films because of the structural versatility and the relative ease by which L−B films are characterized.

The second approach is to attempt kinetic measurements and use the classical nucleation theory outlined above to obtain a value for IFEN. This is then related to other physical properties of the surfaces as well as observation of orientation and selection of particular mineral phases. These studies are more amenable to solid macroscopic substrates such as functionalized polymers and self-assembled monolayers. Generally structural manipulation and characterization of these surfaces is much more difficult, but it is possible to characterize the surfaces phusically with, for example, adsorption isotherm and contact angle wettability studies. This approach emphasizes understanding the interfacial forces driving nucleation rather than the structure of the substrate.

A complete understanding of nucleation at organic interfaces should make use of both approaches. Unfortunately such a synthesis has not been achieved. Further, in many studies, the issue of induction of nucleation by the surface is questionable. Manipulation of mineral phase and crystallographic orientation is possible in these cases, but it is not clear that the surface plays a role in nucleation. Often the observation of unusual mineral phase or crystallographic orientation is taken to infer heterogeneous nucleation—such may not be the case.

Many systems of practical importance involve deposition of minerals under L−B films in which supersatu-

ration is driven by infusion into or effusion of gas from the air-water interface. The formation of metal sulfide films by infusion of H_2S has been extensively studied by Fendler and co-workers.[50] The emphasis of this work has been to prepare monosized metal sulfide particles of sufficiently small size to take advantage of size-quantization effects. The electrical and optical properties of these films are of considerable interest.

Zhao et al. note that CdS and ZnS films form only under negatively charged monolayers and not under positively charged monolayers.[51] They did not find that the negative amphiphile used influenced the film structure. At first, an incomplete monolayer of particles is formed, followed by additional particulate layers to form a three-dimensional porous semiconductor film. More uniform coverage was favored by compressed L−B films. Films in a predominantly fluid state led to disjointed patches of precipitate. In the absence of a monolayer, bulk precipitate is formed. The authors attribute confinement of the mineral film to regions under the L−B film to the strong electrostatic forces between positively charged particles and negatively charged monolayers.

In related work, Yi and Fendler investigated the influence of pH on the surface pressure isotherms of an amine-chelating amphiphile and on subsequent CdS film formation.[52] As pH increased from 6.1 to 9.1, the headgroup area increased and the size of the CdS particles decreased. It is not clear why an increase in spacing of the headgroups leads to a decrease in particulate size. The smallest particulate and most uniform films were formed near pH 9.1, where it has been shown that $Cd(OH)_2$ forms and nucleates CdS formation.[53] The authors claim that the monolayer "templates" semiconductor film formation.

PbS particulate films were formed by Zhao et al.[54] under arachidic acid monolayers. Orientation of the crystals was observed perpendicular to the substrate. More importantly, orientation of the crystals with respect to each other was observed in the plane of the monolayer. This is highly suggestive of an epitaxial relationship; which the authors attributed to the almost perfect match between the 111 plane of the cubic PbS and 100 plane of the hexagonal arachidic acid monolayer. Photographs of the particulate films suggest domains of orientation that hint at corresponding underlying crystalline domains of arachidic acid monolayer.

A similar system is the formation of $CaCO_3$ under L−B films. Deposition occurs under mildly basic conditions where the mineralization reaction is

$$Ca^{2+} + 2HCO_3^- \rightarrow CaCO_3 + H_2O + CO_2$$

where CO_2 is effused at the air−water interface. Alternatively, precipitation may be induced by infusion of the $(NH_4)_2CO_3$ into $CaCl_2$ solutions. Either way, a steep concentration gradient exists at the surface and nucleation occurs at the air-water interface with or without a monolayer. A number of authors have observed that L−B films modulate the habit, phase, and orientation of the crystals formed.

Mann and co-workers have investigated $CaCO_3$ growth under stearic acid, octadecylamine, octadecanol and cholesterol Langmuir monolayers.[55−57] Neutral octadecanol monolayers inhibited mineralization, while the neutral cholesterol monolayers gave results similar to those in the absence of a monolayer. Oriented calcite and vaterite were observed under negatively charged stearic acid monolayers with the particular polymorph depending on solution conditions. The positively charged octadecylamine monolayers gave oriented vaterite. The extent of monolayer compression did not greatly influence the habit or orientation of the crystals. The type of monolayer did influence the rate of nucleation.

These experiments show the dramatic influence of organic surfaces in modifying the nucleation and growth of $CaCO_3$. The structure of the monolayers is a pseudohexagonal packing with an average headgroup spacing of about 5 Å for the carboxylate and amine terminated monomers. Because stereochemical arrangement of the headgroups is unknown, it is difficult to show a clear structural relationship between monolayer and mineral orientation. The apparent lack of influence of monolayer compression suggests that a structural relationship is not important or that the monolayer adapts the needed conformation at the site of nucleation. Orientation of vaterite seems to be ubiquitous regardless of the type of monolayer used and may be related to the growth conditions and to the CO_2 diffusion gradient in particular. Growth of oriented calcite requires a negatively charged surface and the favorable electrostatic interaction with calcium may catalyze the formation of the thermodynamically favored calcite. According to the rule of Ostwald, vaterite should be kinetically favored over calcite. The negatively charged surfaces may enhance the kinetics of calcite formation.

In more recent work Heywood and Mann[58] studied calcite and aragonite growth under sulfate- and phosphonate-terminated *n*-alkyl monolayers. Despite a hexagonal close-packed structure with a headgroup spacing of about 5 Å that is similar to the carboxylate-terminated monolayers, these monolayers gave different crystallographic orientations. This was attributed to an undetermined stereochemical complementarity between monolayer and mineral.

The role of the monolayer in controlling gas diffusion at the air−water interface has not been addressed. This may influence the CO_2 diffusion gradient at the surface and consequently influence nucleation and growth rates. These in turn can influence crystal habit, phase, and orientation. Another point that has been overlooked is the rheology of the monolayers. The mobility of a nucleus or crystal at these interfaces will be dependent on the strength of chemical interaction. At a neutral monolayer, such as cholesterol, or in the absence of a monolayer the nuclei may have greater lateral diffusion, resulting in aggregation, as well as rotational motion. The monolayers may also prevent sedimentation through strong adhesion to the crystal.

Perhaps the most convincing demonstration of the role of geometric and stereochemical epitaxy in growth of $CaCO_3$ is the work by Berman et al.[59] Oriented calcite was grown on polymerized polydiacetylene films. The diacetylene L−B films polymerize in a 2-D crystal with domains up to 3 mm in size. The calcite grew from these films from the (012) plane. All crystals exhibited the same in-plane orientation, despite being separated by many microns. The *a* axis of calcite was oriented along the polymer backbone direction.

$SrSO_4$ and $BaSO_4$ have also been grown under Langmuir monolayers.[60−62] In both cases enhanced nucleation rates and oriented crystals were observed. Geometric matching and proper stereochemical orientation of the monolayer to the crystal lattice was cited as explanation of the results. As above, a good lattice match is assumed between the crystal and the putative hexagonal array of sulfate headgroups. Unfortunately, these experiments do not characterize the structure of the monolayer sufficiently to more than surmise a structural relationship between monolayer and mineral.

The most complete and convincing work addressing a structural relationship between substrate and mineral comes from Leiserowitz, Lahav, and co-workers, but is for a melt crystallization rather than a dilute solution crystallization.[63−66] The degree of supercooling required to induce nucleation of ice from water drops was studied under a wide variety of alcohol monolayers including mixed monolayers. The supercooling required depended strongly on the hydrocarbon backbone length as well as the parity. Grazing incidence X-ray diffraction was used to characterize the monolayers. The backbone length influenced the structure of the monolayer, in particular the tilt of the backbone, and the coherence length of the crystalline domains. The 2−D lattice of the longer-chain alcohols matched closely the lattice hexagonal ice surface. The difference between even and odd chain lengths was attributed to the stereochemical arrangement of the hydroxyl group at the water interface. Studies of mixed and immiscible monolayers provided convincing secondary information to support these conclusions. The detailed structural characterization of the monolayers provides the link that allows a geometric and stereochemical relationship between organic substrate and mineral to be satisfactorily supported.

Far less work has been done on the growth of minerals on solid submerged organic substrates. Solid substrates have the advantage that they can be manipulated easily and characterized by ex situ means. Most future practical applications of mineral deposition will involve some sort of solid substrate.

Preferential and/or oriented growth has been achieved in a number of cases. Zincophosphate zeolite was grown on stacked Zr phosphate monolayers by Feng and Bein.[67,68] Growth occurred from a precipitated zincophosphate mixture or slurry after a 5 h incubation period. They suggest that zeolite nuclei formed in the mixture physisorb to the surface in an oriented manner and subsequently grow to 2 μm. Physisorption and orientation appear to depend on the presence of at least three stacked monolayers.

Campbell et al. explored calcium oxalate deposition on methyl, bromo, thiazolidine, and imidazole-terminated self-assembled monolayers (SAMs).[69] The imidazole monolayer was substantially superior in its ability to nucleate calcium oxalate. They suggest that the orientation of the carboxylate group of the thiazolidine away from the SAM−solution interface make this surface less effective than the imidazole surface.

Hydroxyapatite has been deposited on sulfonate group terminated SAMs on titanium surfaces.[70] The sulfonate SAM is highly effective at promoting mineralization by HAP. The objective of this work was to coat porous titanium bone implant materials and not to understand the details of nucleation at these surfaces (Figure 4).

A number of metal oxides have been deposited on polymer, metal, and ceramic substrates functionalized with various organofunctional groups. These include SnO_2, TiO_2, FeOOH, and MnO_2.[71−73] The objective of this work was to produce functional coating and does not provide an understanding of structural and chemical parameters influencing nucleations. It is, however, interesting to note that one does not have to design a desired structure into a surface specifically to promote mineralization.

The most detailed studies of metal oxide nucleation have been with FeOOH.[74−78] Rieke and co-workers demonstrated that by patterning SAMs with desired functional groups one can pattern the subsequent mineral deposition at resolutions approaching 1.0 μm.[77,78] This work clearly demonstrates the efficacy of sulfonate surface in promoting heterogeneous nucleation. Studies of nucleation kinetics have shown that classical nucleation theory can be used to interpret induction time data and obtain the interfacial free energy for nucleation as defined above.[75] In further nucleation experiments the interfacial free energy of nucleation was determined for mixed SAMs of methyl- and sulfonate-terminated monomers. These data were compared with the surface composition, the adsorption of iron, and the work of water adhesion to the SAMs. At low percentage sulfonate, a good correlation between the IFEN and these data was obtained. However, at high percentage sulfonate monomer, the data were essentially independent of these parameters and this effect remains unexplained.[76] Figure 5 shows selective FeOOH deposition on a sulfonated SAM but not on adjacent hydrophobic SAM.

In part it is not clear from a theoretical perspective how composition, cation adsorption, or wettability relate to the IFEN. The work of Van Oss and Good regarding measurement of individual surface free energies and the decomposition of these into acid, base, and Lifshitz−van der Waals contributions can be used in combination with nucleation theory to overcome partially this problem.[30,31] Further this data represents only one example of careful solution nucleation kinetics studies on macroscopic surfaces. Such experiments must be repeated for other minerals.

Precipitation in Polymers

In principle, biomineralization processes involve both mineralization on a polymeric substrate and mineralization in a polymeric matrix. However, as will be shown below, the distinction is not always clear. The surfaces of partly hydrophilic polymers are diffuse and growth on a surface may be preceded by subsurface nucleation.

In situ precipitation in polymer films can be carried out by blending a polymer or polymer precursor with a soluble inorganic reagent which subsequently precipitates. For instance, metal alkoxides can be blended with polymers or monomers and then hydrolyzed to form metal oxide. The formation of the polymer and of the oxide can occur concurrently or sequentially. Calvert has recently reviewed this area in detail.[3] In most of these cases the polymer does not take an active part in the precipitation but nonetheless controls the process through phase behavior, diffusion effects and matrix orientation.

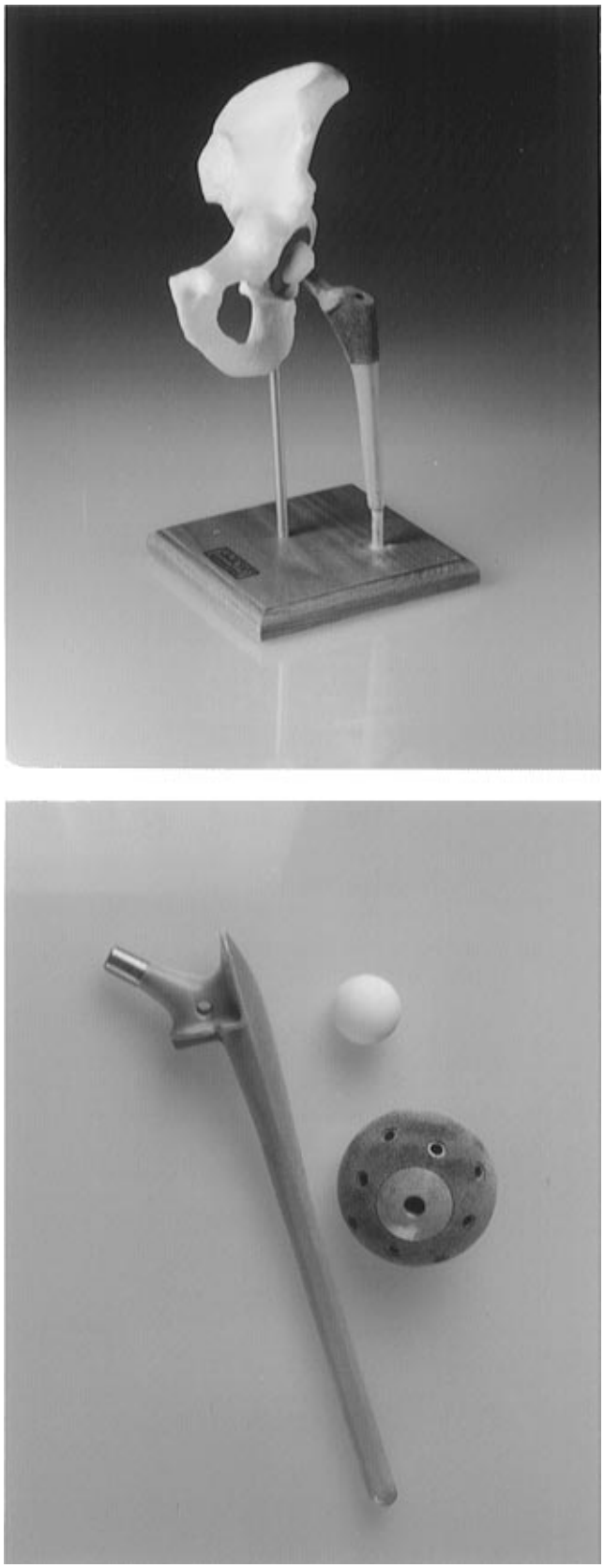

Figure 4. Titanium hip implant coated with a thin, coherent hydroxyapatite layer.

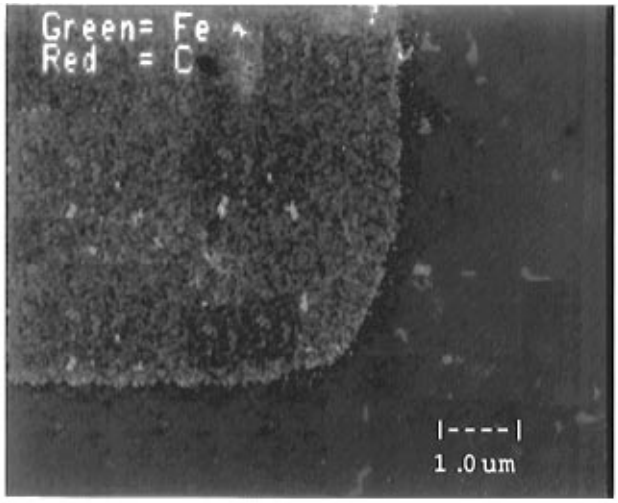

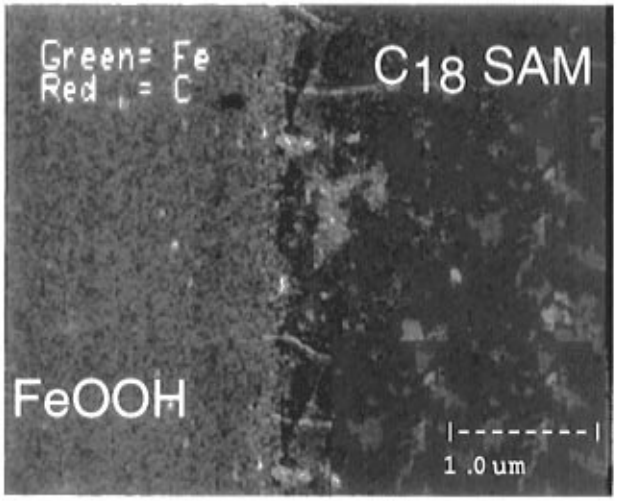

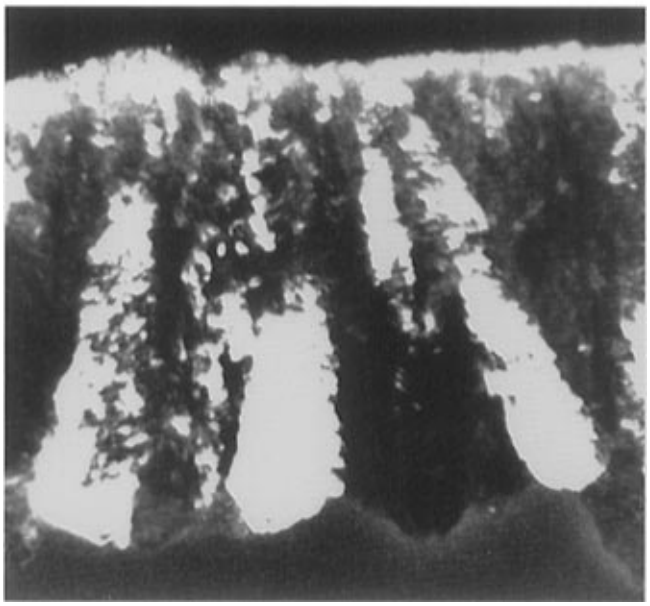

Figure 5. Selective deposition on FeOOH on a silicon substrate. Sulfonated SAM mineralizes, but the hydrophobic area does not: (a) surface; (b) cross section.

The archetypal organic−inorganic hybrid could be taken to be silica-filled poly(methyl methacrylate). This is a combination of conventional polymer chemistry with sol−gel chemistry such as the hydrolysis and condensation of a silicon tetraethoxide to silica. The most straightforward approach is to blend the polymer, alkoxide, and water into a mutual solvent such as THF, cast a film, and allow it to react and dry. The total silica content of such materials is limited to about 20 vol % which corresponds to about 60 vol % alkoxide in the starting alkoxide/polymer mixture.

These materials show the property changes that would be expected for an equivalent filled polymer composite. The elastic modulus (stiffness) increases, the strength may go up or down, but the elongation to break and toughness decrease. As predicted, the increase for hard polymers is less than 50% at 20 vol % silica. A stiffness change of several-fold would be needed before these materials were of interest as stiffer molding materials to replace polymers. As might be expected, the impregnated sol−gel composites, which are interpenetrating networks of organic and inorganic phases, are much stiffer and glasslike than the polymer-matrix materials.

Hybrids can be formed by a number of routes. As described above, a solution of poly(methyl methacrylate) can be mixed with a liquid silicon alkoxide and allowed to dry, and then the trapped alkoxide hydrolyzed to silica. Methyl methacrylate monomer may be mixed with alkoxide and polymerized, and then the silica formed by hydrolysis. A solution of alkoxide in alcohol can be hydrolyzed to form porous silica which is then impregnated with methyl methacrylate, followed by polymerization. The polymerization and hydrolysis can also be run simultaneously. It has been argued that this minimizes the extent of phase separation and produces a transparent composite.[79]

In addition to silica, many other reinforcing or active phases have been introduced into polymers. Successful hybrids have been formed with titania, zirconia, barium titanate, iron oxides, and other oxides.[80−82] Sulfides can be formed by incorporating a metal compound into the polymer and then exposing the material to hydrogen sulfide or a reactive sulfur compound such as bis-(trimethylsilyl)sulfur.[83] Metals can be incorporated by reduction of a polymer-bound metal salt with hydrogen, sodium naphthalide or borohydride. Metals compounds such as carbonyls can also be thermally decomposed in situ.[84,85] Platinum, silver, and gold have also been formed by photodecomposition of metal salts.

The core argument for making composites by in situ precipitation is that the particle size, shape and distribution can be controlled. Composites with large particles, randomly distributed, can always be made by blending of the polymer and filler.

Particle Size Control. The particle size of the reinforcement is sensitive to the precipitation rates and conditions. One sensitive test is transparency, where a transparent composite implies that phase separation has occurred on a scale of less than 100 nm. A general belief that better properties will result from nanometer-size reinforcements has driven workers toward transparent composites.

If we consider a cast film of polymer, solvent, and alkoxide, the system may follow a number of paths as the solvent evaporates and hydrolysis occurs.[86] In a dry system, the most likely event is that loss of solvent will result in a phase separation of alkoxide plus solvent from the polymer. If the compatibility is good and the alkoxide level low, this will occur when there is little solvent left and the film is nearly rigid. As a result the separation will occur on a very fine scale. Subsequent hydrolysis and condensation will convert the trapped alkoxide droplets to oxide particles. If the alkoxide is very compatible with the polymer, the separation will not occur until the hydrolysis takes place. The particle size will then depend on the balance of reaction rate and diffusion rate. Although the factors controlling this process are evident, no system has been developed to the point of interpreting the microstructural development in detail and the phase separation theories have not been formally applied.

There have recently been some interesting observations on the effect of matrix cross-link density and molecular weight on silica particle size for silicone rubber−silica composites as determined by small-angle neutron scattering. The particle size is found to vary with the square root of the molecular weight between cross-links, implying that the silica particle growth is limited by the degree of expansion available to the rubber chains surrounding the particles.[87]

Interfacial Bonding. In hybrid systems where a low molecular weight polymer is blended with alkoxide, it has been shown that the polymer should contain groups capable of reacting with the inorganic network. Thus silica−polyether hybrids have been coupled with terminal alkoxy groups on the polymer.[88,89] This reaction may function both to provide good interfacial bonding and to restrict the scale of the phase separation by forming a cross-linked network. Systems that have poor interfacial bonding do seem to have very poor mechanical properties, but there is no sign of improved properties due to stronger interfacial bonding over some minimum corresponding to polar interactions.

Particle Shape Control. For filled polymers, much better properties are obtained with fibrous fillers, especially if the axial ratio is greater than 10. This suggests that better hybrids could be formed by growing elongated particles in situ. A number of studies have shown how this might be done, but there is as yet no unequivocal proof of better strength properties.

Okada and co-workers[90] and Giannelis and co-workers[91,92] have developed hybrids of montmorillonite clays and thermoplastics. These clays have a layered crystal structure wherein the individual layers can be separated by treatment with a cationic amphiphile (detergent). Okada has characterized composites of clay layers with nylon 6[93] and polyimide.[94] These composites show a much increased stiffness at low volume fractions of clay, but are still substantially more brittle than the base polymer.

Elongated particles have been formed by in situ growth of titania in oriented polymer films.[95] In this case the polymer containing titanium alkoxide is hot drawn and then treated to hydrolyze the alkoxide. Efforts to produce elongated particles by swelling alkoxide into an oriented polymer film were unsuccessful. However a two-phase blend of poly(vinylidene fluoride) and poly(methyl methacrylate) could be swollen such that the alkoxide entered the acrylic phase and, on hydrolysis, precipitated in a form resembling a row of peas in a pod. Schrock and co-workers have formed two-phase block copolymers where one phase can be doped with a metal ion which is then converted to metal, oxide, or sulfide.[96]

In a similar effort to form oriented particles by using the polymer morphology as a mold, titania has been incorporated into polypropylene by melt blending with alkoxide, extrusion, and hydrolysis. It was expected that the particles would be limited to the amorphous regions between the lamellar crystallites. While this

probably occurred, titanium alkoxide also segregated to spherulite boundaries where it formed a brittle zone.[97] Mauritz and co-workers have grown silica in two-phase Nafion membranes by an impregnation and hydrolysis method.[98]

Clearly it should be possible to form elongated particles in polymers by in situ growth of anisotropic crystals. This has been achieved for organic fillers,[99] but no reinforcing whiskers have been produced in situ.

Mineralization. Most of the materials mentioned above are formed by mixing one component with the polymer and then reacting it in place. It would be attractive to devise a mineralization system where the reagents would diffuse into the polymer either at once or sequentially. In principle this allows mineralization of existing shapes and allows higher volume fractions to be reached through several cycles of impregnation and reaction. Vapor-phase swelling has been used by Mark and co-workers[100] to impregnate silicone rubber with silicon tetraethoxide which is subsequently hydrolyzed. These materials have been extensively characterized.

We have formed surface-hardened polyester films in this way by diffusing silicon tetraisocyanate into sheets and then reacting this with moisture.[8] We have also reinforced copolymers of ethylene and aminated acrylates by amine catalysis of silica sols.[101] A metastable acidic silica sol is formed and allowed to diffuse into the basic polymer matrix where it precipitates as silica. Neither approach is easily generalized, as it requires a polymer matrix which is heavily swollen by all components of the reacting mixture without dissolution or degradation and, in the second case, which carries groups catalytic for the reaction. We had initially believed that most reagents could be impregnated into a polymer by the use of a strongly swelling co-solvent. Experience has taught us that this is usually untrue and the reagent does not follow the solvent into the polymer.

Cadmium sulfide layers have been formed in acrylate polymers by overcoating a cadmium acetate-doped poly(methyl methacrylate) layer with a thioacetamide-doped film of poly(acrylic acid). Heating this sandwich gives rise to a cadmium sulfide layer at the interface, after which the polyacrylic acid layer can be washed off in water to leave a surface film of mineral.

One true analogue of biomineralization would be a polymer matrix which can be placed into a metastable solution and induce precipitation to occur within the polymer but not in the solution. Such a material could then be left in the solution to mineralize. This problem is clearly related to that of mineralization on polymer surfaces which was discussed above. We have found that certain hydroxylated acrylates will mineralize in a calcium oxalate solution, while very little precipitation occurs in the surrounding liquid and none is observed until much later in a similar solution with no polymer film.[42,46] The effect is specific in that many related acrylates, including various acidic copolymers, were not effective. The crystal morphology also varied with polymer composition. Table 1 lists a series of insoluble acrylate copolymers which were tested for mineralization by oxalate. Apparently, nucleation of oxalate crystals actually occurs at the interface between the polymer and the underlying glass substrate and the crystal then grows up through the film and into the solution (Figure 6).

Table 1. Oxalate Mineralization of Copolymer Films[a]

copolymer	result (no entry: no effect)
10% MAA, 90% THFFMA	
10% THFFMA, 90% butyl MA	
50% MAA, 50% THFFMA	dissolves
20% MAA, 80% THFFMA	
30% MAA, 70% THFFMA	cloudy in DI water
20% MAA, 80% butyl MA	
40% MAA, 60% THFFMA	
20% THFFMA, 80% butyl MA	
30% MAA, 70% butyl MA	some surface crystallization
20% HEMA, 80% THFFMA	
80% HEMA, 20% THFFMA	surface crystallization
20% MAA, 80% ethoxy	
50% ethoxy, 50% butyl MA	
50% Ethoxy, 50% THFFMA	
80% HEMA, 20% MAA	insoluble, intractable polymer
60% HEMA, 40% MAA	insoluble, intractable polymer
80% HEMA, 20% butyl MA	
80% HEMA, 20% ethoxy	
50% MAA, 50% butyl MA	dissolves
80% HBA, 20% THFFMA	surface crystallization
80% HPMA, 20% THFFMA	surface crystallization
80% HPA, 20% THFFMA	surface crystallization

[a] MAA, methyacrylic acid; butyl MA, butylmethacrylate; THFFMA, tetrahydrofurfuryl methacrylate; ethoxy, 2-ethoxyethyl methacrylate; HEMA, 2-hydroxyethyl methacrylate; HPA, 3-hydroxypropyl acrylate; HPMA, 3-hydroxypropyl methacrylate; HBA, 4-hydroxybutyl acrylate.

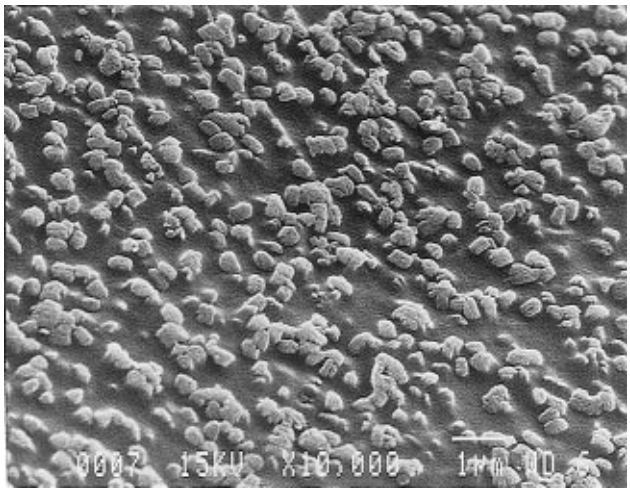

Figure 6. Calcium oxalate mineralization on a film of hydroxyethylmethacrylate−tetrahydrofurufalmethacrylate (80:20) copolymer, after 30 min of growth in 4.5×10^{-4} M solution of calcium oxalate at pH 10.4 plus 50 ppm of polyacrylic acid.[46]

$CaCO_3$ has also been grown on a number of protein-derivatized and synthetic solid substrates. Addadi et al. demonstrated that sulfonated polystyrene substrate upon which polyaspartic acid was physisorbed induced a greater density of oriented calcite than either sulfonated polystyrene or physisorbed polystyrene alone.[102] They attribute this cooperativity to the strong electrostatic attraction of calcium to the sulfonate groups, in combination with the ordered, albeit weaker, binding of calcium by the β-sheet structure of the polyaspartic acid. Greenfield et al. term this effect "ionotropy".[103] These authors demonstrated that shell matrix from Nautilus pompilius, prepared with the hydrophillic sulfonated binding site intact, nucleated spherulitic (presumably vaterite) $CaCO_3$ in vitro. While this work apparently reflects nucleation on a polymer surface, it should be recalled that these acidic polymers, including

surface-sulfonated polystyrene, will form a highly water-swollen layer.

In work that calls into question the role of the surfaces in nucleation, Rieke demonstrated oriented growth of vaterite on polystyrene and calcite on glass.[25,104] Nucleation, however, occurred spontaneously in solution and the nuclei physisorbed to the substrates. The negatively charged glass surface promoted calcite growth similar to the above work under negatively charged Langmuir monolayers. Others have suggested that amorphous $CaCO_3$ nuclei may be kinetically favored and that a major role of the surface is in phase transformation.[105,106] Presumably glass promotes a phase transformation to calcite while polystyrene does not. The relevance here is that observation of phase selection or crystallographic orientation does not necessarily imply selective nucleation. Nor are specific structural relationships between the nuclei and substrate necessary to achieve orientation. Electrostatic and van der Waals forces involved in colloid physisorption may be just as important.

The importance of solid−solid interfaces below a swollen polymer layer seems to be reinforced by the recent work of Falini et al. showing that two solid polymers and a soluble glycoprotein are necessary for regeneration of the correct polymorph of calcite on polymers extracted from mollusc shell.[107] Falini et al. demonstrated that macromolecules extracted from the aragonitic and calcitic portion of molluskan shell were able to induce in vitro aragonite and calcite growth respectively when immobilized upon β-chitin and silk fibroin. Aragonite has not previously been demonstrated to grow on substrates in the absence of Mg^{2+}.

Conclusions

Simple heterogeneous nucleation arguments have dominated discussion of mineralization processes for some time. We have argued here that local control of concentration and inhibition are at least as important. We also show that epitaxy on a solid surface is not an appropriate description for crystal growth originating in or on a soft, flexible polymer layer.

As demonstrated recently, simple surface mineralization of insoluble materials is limited to very slow deposition in a narrow concentration window. These rates can be increased and the window widened by manipulation of the solution chemistry, but very careful control of conditions is still necessary. As we learn more about the role of biological macromolecules in mineralization processes, we will learn how to make synthetic surface mineralizations more robust. Given this understanding, there is a range of potential applications for this approach.

As originally conceived, organic−inorganic hybrids were expected to deliver properties superior to those of filled polymers by virtue of their nanometer particle size. However, this plausible belief is not supported by simple composite theory which contains no size-dependent terms in calculations of strength or modulus. In the case of fiber-reinforced composites, fracture energy would be expected to increase as fibre diameter increased.[108] Now that we have some mechanical data on hybrids, the theory has been borne out.

If we return to bone as a prototype for a composite with good toughness and stiffness properties, we have reproduced many of the characteristics of bone. Nanometer reinforcements grown by in situ mineralization were not the sole answer. Poor interfacial bonding has been shown to lead to very poor properties, but there is no reason to expect that especially strong bonding will lead to especially high strengths. Nanosized, elongated particles have been used in the clay hybrids without giving great toughness, but it is conceivable that in situ growth of more rodlike particles may give a real improvement.

One characteristic of bone that has not been incorporated is the structural hierarchy. Bone and tooth are tough due to microfracturing rather than yield and flow.[109] It may be that this is a function of planes of weakness in the material rather than the properties of the homogeneous matrix. This concept is being explored by a number of workers for ceramics.[110−112] If this is true, toughness of hybrids will come from structural manipulation at the scale of microns and above, in addition to the stiffness due to fine scale reinforcement.

The growth of dense, fine-grained films on polymer surfaces offers the possibility for improving the hardness and permeation resistance of plastics. It also may allow us to form devices which would complement silicon technology.

Acknowledgment. P.C. would like to thank the Air Force Office of Scientific Research and the Army Research Office for support of work on biomineralization. Research at the Pacific Northwest Laboratory is supported by the DOE, Office of Basic Energy Sciences.

References

(1) Calvert, P. In *Biomimetics*; M. Sarikaya and I. A. Aksay, Ed.; AIP Press: Woodbury, NY, 1995; pp 145.
(2) Currey, J. D.; Zioupos, P. ; Sedman, A. In *Biomimetics*; Sarikaya, M., and Aksay, I. A., Eds.; AIP Press: Woodbury, NY, 1995; p 117.
(3) Calvert, P. D. In *Biomimetic Materials Chemistry*; Mann, S., Ed.; VCH Publishers: Weinheim, Germany, 1996; p 315.
(4) Mann, S.; Webb, J.; Williams, R. J. P. *Biomineralization: chemical and biochemical perspectives*; VCH: Weinheim, 1989.
(5) Calvert, P. In *International Encyclopedia of Composites*; Lee, S. M., Ed.; VCH Publishers: Weinheim, Germany, 1991; Vol. 6.
(6) Wang, B.; Wilkes, G. L. *J. Macromol. Sci.—Pure Appl. Chem.* **1994,** *31*, 249.
(7) Kasemann, R.; Schmidt, H. *New J. Chem.* **1994,** *18*, 1117.
(8) Lombardi, J. L.; Calvert, P. D. In *Materials Research Society Symposium Proceedings, Nanophase and Nanocomposite Materials Symposium*; Komarneni, S., Parker, J. C., Thomas, G. J., Ed.; Materials Research Society: Pittsburgh, PA, 1993; Vol. 286, p 309.
(9) Gladfelter, W. L. *Chem. Mater.* **1993,** *5*, 1372.
(10) Constantz, B. R. *Palios* **1986,** *1*, 152.
(11) Doyle, R. J.; Taylor, K. G. *Cells Mater.* **1994,** *4*, 91.
(12) Arends, J. In *Biological Mineralization and Demineralization: Dahlem Conference*; Nancollas, G. H., Ed.; Springer-Verlag: Berlin, 1982; p 303.
(13) Awramik, S. M. *Photosynth. Res.* **1992,** *33*, 75.
(14) Keller, A.; Hikosaka, M.; Rastogi, S.; Toda, A.; Barham, P. J.; Goldbeck-Wood, G. *J. Mater. Sci.* **1994,** *29*, 2579.
(15) Lowenstam, H. A.; Weiner, S. *On Biomineralization*; Oxford University Press: Oxford, 1989.
(16) Weiner, S.; Traub, W. *FASEB J.* **1992,** *6*, 879.
(17) Fleisch, H. In *Biological Mineralization and Demineralization*; Nancollas, G. H., Ed.; Springer-Verlag: Berlin, 1982; p 233.
(18) Bianco, P. In *Calcification in Biological Systems*; Bonucci, E., Ed.; CRC Press: Boca Raton, FL, 1992.
(19) Fritz, M.; Belcher, A. M.; Radmacher, M.; Walters, D. A.; Hansma, P. K.; Stuckey, G. D.; Morse, D. E.; Mann, S. *Nature* **1994,** *371*, 49.
(20) Jackson, A. P.; Vincent, J. F. V.; Turner, R. M. *J. Mater. Sci.* **1990,** *25*, 3173.
(21) Garrone, R.; Simpson, T. L.; Pottu-Boumendil, P. In *Silicon and Siliceous Structures in Biological Systems*; Simpson, T. L., Volcani, B. E., Ed.; Springer: Berlin, 1981; p 495.
(22) Nancollas, G. H. *Adv. Colloid Interface Sci.* **1979,** *10*, 215.

(23) Dieppe, P. A.; Calvert, P. D. *Crystals and Joint Disease*; Chapman and Hall: London, 1983.
(24) Heywood, B. R.; Mann, S. *Adv. Mater.* **1994,** *6*, 9.
(25) Rieke, P. C. *Mat. Sci. Eng., C, Biomimetic Mater. Sensors Systems*, in press.
(26) Nielsen, A. E. *Kinetics of precipitation*; Macmillan: New York, 1964.
(27) Nyvlt, J.; Sohnel, O.; Matuchova, M.; Broul, M. *The kinetics of industrial crystallization*; Elsevier: Amsterdam, 1985.
(28) Tiller, W. A. *The science of crystallization, p.342*; Cambridge University Press: Cambridge, 1991; p 342.
(29) Walton, A. G. *The formation and properties of precipitates*; Interscience: New York, 1967.
(30) Berg, J. C. In *Wettability*; Berg, J. C., Ed.; Marcel Dekker: New York, 1993; p 75.
(31) Good, R. J.; Oss, C. J. v. In *Modern Approach to Wettability*; Schrader, M. E., G. Loeb, G., Eds.; Plenum: New York, 1991.
(32) Jackson, K. A.; Uhlmann, D. R.; Hunt, J. D. *J. Cryst. Growth* **1967,** *1*, 1.
(33) Burton, W. K.; Cabrera, N. *Discuss. Faraday Soc.* **1949,** *5*, 33.
(34) Venables, J. A.; Smith, B. L. In *Rare Gas Solids*; Klein, M. L., Venables, J. A., Eds.; Academic Press: London, 1977; Vol. 2, p 609.
(35) Doremus, R. H.; Roberts, B. W.; Turnbull, D. *Growth and perfection of crystals*; Wiley: New York, 1958.
(36) Hillner, P. E.; Manne, S.; Hansma, P. K.; Gratz, A. J. *Faraday Discuss.* **1993,** *95*, 191.
(37) Hillner, P. E.; Manne, S.; Gratz, A. J.; Hansma, P. K. *Ultramicroscopy* **1992,** *42−44*, 1387.
(38) Nielsen, A. E. *J. Cryst. Growth* **1984,** *67*, 289.
(39) Nielsen, A. E.; Toft, J. M. *J. Cryst. Growth* **1984,** *67*, 278.
(40) Jancic, S. J.; Grootscholten, P. A. W. *Industrial Crystallization*; Reidel: Hingham, MA, 1984.
(41) Oner, M.; Calvert, P. *Mater. Sci. Eng. C* **1994,** *2*, 93.
(42) Calvert, P. *Mater. Res. Soc. Symp. Proc.* **1994,** *330*, 79.
(43) Mann, S.; Heywood, B. R.; Rajam, S. 1 *Nature* **1988**, 693.
(44) Davey, R. J.; Black, S. N.; Bromley, L. A.; Cottier, D.; Dobbs, B.; Rout, J. E. *Nature* **1991,** *353*, 549.
(45) Black, S. N.; Bromley, L. A.; Cottier, D.; Davey, R. J.; Dobbs, B.; Rout, J. E. *J. Chem. Soc., Faraday Trans.* **1991,** *87*, 3409.
(46) Burdon, J.; Oner, M.; Calvert, P. *Mater. Sci. Eng., C*, in press.
(47) Zhang, S. K.; Gonsalves, K. E. *J. Appl. Polym. Sci.* **1995,** *56*, 687.
(48) Crenshaw, M. A.; Linde, A.; Lussi, A. In *Atomic and Molecular Processing of Electronic and Ceramic Materials*; Aksay, I. A., McVay, G. L., Wager, J. F., Eds.; Materials Research Society: Pittsburgh, PA, 1987; p 99.
(49) Tsao, J. Y. *Materials fundamentals in molecular beam epitaxy*; Academic Press: San Diego, 1993.
(50) Fendler, J. H.; Meldrum, F. C. *Adv. Mater.* **1995,** *7*, 607.
(51) Zhao, X. K.; Xu, S.; Fendler, J. H. *Langmuir* **1991,** *7*, 520.
(52) Yi, K. C.; Fendler, J. H. *Langmuir* **1990,** *6*, 1519.
(53) Rieke, P. C.; Bentjen, S. B. *Chem. Mater.* **1993,** *5*, 43.
(54) Zhao, X. K.; Yang, J.; McCormick, L. D.; Fendler, J. H. *J. Phys. Chem.* **1992,** *96*, 9933.
(55) Mann, S.; Heywood, B. R.; Rajam, S.; Birchall, J. D. *Proc. R. Soc. London A* **1989,** *423*, 457.
(56) Mann, S.; Heywood, B. R.; Rajam, S.; Walker, J. B. W. *J. Phys. D: Appl. Phys.* **1991,** *3*, 154.
(57) Rajam, S.; Heywood, B. R.; Walker, J. B. A.; Mann, S.; Davey, R. J.; Birchall, J. D. *J. Chem. Soc., Faraday Trans.* **1991,** *87*, 727.
(58) Heywood, B. R.; Mann, S. *Chem. Mater.* **1994,** *6*, 311.
(59) Berman, A.; Ahn, D. J.; Lio, A.; Salmeron, M.; Reichert, A.; Charych, D. *Science* **1995,** *269*, 515.
(60) Heywood, B. R.; Mann, S. *Langmuir* **1992,** *8*, 1492.
(61) Heywood, B. R.; Mann, S. *J. Am. Chem. Soc.* **1992,** *114*, 4681.
(62) Hughes, N. P.; Heard, D.; Perry, C. C. ; Williams, R. J. P. *J. Phys. D: Appl. Phys.* **1991,** *24*, 146.
(63) Majewski, L.; Popovitz-Biro, R.; Kjaer, K.; Als-Nielsen, J.; Lahav, M.; Leiserowtiz, L. *J. Phys. Chem.* **1994,** *98*, 4087.
(64) Gavish, M.; Popovitz-Biro, R.; Lahav, M.; Leiserowitz, L. *Science* **1990,** *250*, 973.
(65) Popovitz-Biro, R.; Wang, J. L.; Majewski, J.; Shavit, E.; Leiserowitz, L.; Lahav, M. *J. Am. Chem. Soc.* **1994,** *116*, 1179.
(66) Wang, R.; Leveiller, F.; Jacquemain, D.; Kjaer, K.; Als-Nielsen, J.; Lahav, M.; Leiserowitz, L. *J. Am. Chem. Soc.* **1994,** *116*, 1192.
(67) Feng, S.; Bein, T. *Nature* **1994,** *368*, 834.
(68) Feng, S.; Bein, T. *Science* **1994,** *265*, 1839.
(69) Campbell, A. A.; Fryxell, G. E.; Graff, G. L.; Rieke, P. C.; Tarasevich, B. J. *Scanning Microsc.* **1993**, 423.
(70) Campbell, A. A.; Graff, G. L.; Fryxell, G. E.; Miller, G. J.; Wheeler, D. L. *J. Biomed. Mater. Res.*, in press.
(71) Bunker, B. C.; Rieke, P. C.; Tarasevich, B. J.; Campbell, A. A.; Fryxell, G. E.; Graff, G. L.; Song, L.; Liu, J.; Virden, J. W.; McVay, G. L. *Science* **1994,** *264*, 48.
(72) Rieke, P. C.; Tarasevich, B. J.; Bentjen, S. B.; Fryxell, G. E.; Campbell, A. A. In *Supramolecular Architecture*; Bein, T., Ed.; American Chemical Society: Washington, DC, 1992; Vol. 499, p 61.
(73) Rieke, P. C.; Graff, G. E.; Campbell, A. A.; Bunker, B. C.; Baskaran, S.; Song, L.; Tarasevich, B. J.; Fryxell, G. E. In *Challenging to Future Advanced Materials Aiming For Intelligence and Harmonization*; Maekawa, Z., Nakata, E., Sakatani, Y., Eds.; Society for the Advancement of Material and Process Engineering: Yokohama, Japan, 1995; p 565.
(74) Tarasevich, B. J.; Rieke, P. C.; Liu, J. *Chem. Mater.*, in press.
(75) Rieke, P. C.; Marsh, B. D.; Wood, L. L.; Tarasevich, B. J.; Liu, J.; Song, L.; Fryxell, G. E. *Langmuir* **1995,** *11*, 318.
(76) Rieke, P. C.; Wiecek, R. J.; Marsh, B. D.; Wood, L. L.; Liu, J.; Song, L.; Fryxell, G. E.; Tarasevich, B. J. *Langmuir*, in press.
(77) Rieke, P. C.; Tarasevich, B. J.; Wood, L. L.; Marsh, B. M.; Fryxell, G. E.; Engelhard, M. H.; Baer, D. R.; John, C. M. In *Fall 1993 Materials Reseach Society Meeting Boston, MA, "Biomolecular Materials by Design"*, 1993.
(78) Rieke, P.; Tarasevich, B.; Wood, L.; Engelhard, M.; Baer, D.; Fryxell, G.; John, C.; Laken, D.; Jaehnig, M. *Langmuir* **1994,** *10*, 619.
(79) David, I. A.; Scherer, G. W. *Polym. Prepr.* **1991,** *32*, 530.
(80) Calvert, P. D.; Broad, R. A. In *Contemporary Topics in Polymer Science*; Culbertson, B. M., Ed.; Plenum: New York, 1989; Vol. 6, p 95.
(81) *MRS Symposia Materials Synthesis Utilizing Biological Processes*; Rieke, P. C., Calvert, P. D., Alper, M., Eds.; Materials Research Society: Pittsburgh, PA, 1990; Vol. 174, p 61.
(82) Brennan, A. B.; Wang, B.; Rodrigues, D. E.; Wilkes, G. L. *J. Inorg. Organomet. Polym.* **1991,** *1*, 167.
(83) Bianconi, P. A.; Lin, J.; Strelecki, A. R. *Nature* **1991,** *349*, 315.
(84) Nandi, M.; Conklin, J. A.; L. Salvati, J.; Sen, A. *Chem. Mater.* **1990,** *2*, 772.
(85) Tannenbaum, R.; Flenniken, C. L.; Goldberg, E. P. *J. Polym. Sci., Polym. Phys.* **1987,** *25*, 1341.
(86) Burdon, J.; Calvert, P. *Mater. Res. Soc. Symp. Proc.* **1993,** *286*, 315.
(87) Ulibarri, T. A.; Beaucage, G.; Schaefer, D. W.; Oliver, B. J.; Assink, R. A. *Mater. Res. Soc. Symp. Proc.* **1992,** *274*, 85.
(88) Wilkes, G. L.; Huang, H.-H.; Glaser, R. H. In *Silicon-Based Polymer Science*; Ziegler, J. M., Fearon, F. W. G., Eds.; American Chemical Society: Washington, DC, 1990; Vol. 224, p 207.
(89) Boulton, J. M.; Fox, H. H.; Neilson, G. F.; Uhlmann, D. R. *Mater. Res. Soc. Symp. Proc.* **1990,** *180*, 773.
(90) Usuki, A.; Kojima, Y.; Kawasumi, M.; Okada, A.; Fukushima, Y.; Kurauchi, T.; Kamigaito, O. *J. Mater. Res.* **1993,** *8*, 1179.
(91) Messersmith, P.; Giannelis, E. *Chem. Mater.* **1993,** *5*, 1064.
(92) Messersmith, P.; Giannelis, E. *Chem. Mater.* **1994,** *6*, 1719.
(93) Kojima, Y.; Usuki, A.; Kawasumi, M.; Okada, A.; Kurauchi, T.; Kamigaito, O.; Kaji, K. *J. Polym. Sci. Phys.* **1994,** *32*, 625.
(94) Yano, K.; Usuki, A.; Okada, A.; Kurauchi, T.; Kamigaito, O. *J. Polym. Sci. A* **1993,** *31*, 2493.
(95) Burdon, J.; Calvert, P. D. In *MRS Symposium Hierarchically Structured Materials*; Aksay, I., Baer, E., Sarikaya, M., Tirrell, D. A., Eds.; Materials Research Society: Pittsburgh, PA, 1992; Vol. 255, p 375.
(96) Tassoni, R.; Schrock, R. R. *Chem. Mater.* **1994,** *6*, 744.
(97) Calvert, P.; Burdon, J. *ACS PMSE Prepr.* **1994,** *70*, 224.
(98) Mauritz, K. A.; Warren, R. M. *Macromolecules* **1989,** *22*, 1730.
(99) Jeska, J. K.; Ulanski, J.; Kryszewski, M. *Nature* **1981,** *289*, 390.
(100) Mark, J. E.; Jiang, C.-Y.; Tang, M.-Y. *Macromolecules* **1984,** *17*, 2613.
(101) Burdon, J. W.; Calvert, P. D. *Mater. Res. Soc. Symp. Proc.* **1991,** *218*, 203.
(102) Addadi, L.; Moradian, J.; Shay, E.; Maroudas, N. G.; Weiner, S. *Proc. Natl. Acad. Sci. U.S.A.* **1987,** *84*, 2732.
(103) Greenfield, E. M.; Wilson, D. C.; Crenshaw, M. A. *Am. Zool.* **1984,** *24*, 925.
(104) Rieke, P. C. In *Atomic and Molecular Processing of Electronic and Ceramic Materials*; Aksay, A. I., McVay, G. L., Stoebe, T. G., Wager, J. F., Eds.; Materials Research Society: Pittsburgh, PA, 1987; p 109.
(105) Mann, S. *Struct. Bonding* **1983,** *54*, 125.
(106) Simkiss, K. *Am. Zool.* **1984**, *24*, 847.
(107) Falini, G.; Albeck, S.; Weiner, S. ; Addadi, L. *Science* **1996,** *271*, 87.
(108) Hull, D. *Introduction to Composites*; Cambridge University Press: Cambridge, 1981.
(109) Currey, J. D. *The Mechanical Adaptions of Bones*; Princeton University Press: Princeton, 1984.
(110) Clegg, W. J.; Kendall, K.; Alford, N. M.; Button, T. W.; Birchall, J. D. *Nature* **1990,** *347*, 455.
(111) Baskaran, S.; Nunn, S. D.; Popovic, D.; Halloran, J. W. *J. Amer. Ceram. Soc.* **1993,** *76*, 2209.
(112) Folsom, C. A.; Zok, F. W.; Lange, F. F.; Marshall, D. B. *J. Am. Ceram. Soc.* **1992,** *75*, 2969.

CM960126O